Kovove Mater. 60 2022 139–150
DOI: 10.31577/km.2022.3.139

Experimental study on rapid evaluation of modification effect of hypoeutectic Al-Si alloy based on melt solidification process resistivity monitoring

Ao Wang[1], Jianming Dong[1], Dayong Li[1,2]*

[1] *School of Materials Science and Chemical Engineering, Harbin University of Science and Technology, Harbin 150040, P. R. China*
[2] *Key Laboratory of Advanced Manufacturing and Intelligent Technology, Ministry of Education, Harbin University of Science & Technology, Harbin 150040, P. R. China*

Received 30 December 2021, received in revised form 11 May 2022, accepted 11 May 2022

Abstract

In order to improve the accuracy of rapid evaluation of the modification effect of Al-Si alloy in front of the furnace, the relationship between resistivity change and modification level during melt solidification was experimentally studied. A melt resistivity monitoring system was designed for practical application, including a sample cup, sample cup base support, vacuum aspiration unit, constant current power supply, data acquisition module, and computer. The monitoring system was used to monitor the changes in temperature and resistivity parameters during solidification of ZL101A alloy melt treated with different amounts of Sr modifier. It was found that the curve of melt resistivity changes with temperature at the eutectic solidification stage had a plateau, and the resistivity plateau value decreased with the better alloy modification effect. Therefore, a rapid evaluation model was established of the hypoeutectic Al-Si alloy modification effect in front of the furnace based on resistivity change during melt solidification. The experimental results showed that the evaluation of the modification effect of the hypoeutectic Al-Si alloy could be completed within 3 minutes by using the monitoring system and evaluation model designed in this paper. The accuracy of the evaluation of modification level error within ± 0.5 reaches 80 % taking the metallographic observation method as the standard.

K e y w o r d s: resistivity, monitoring device, hypoeutectic Al-Si alloys, modification effect, rapid evaluation

1. Introduction

The hypoeutectic Al-Si alloys have been widely used in the automotive and aerospace industry due to their low density, high strength, and good fluidity [1, 2]. However, when the eutectic silicon phase of the alloy is not modified, it is easy to form coarse acicular and flake structures, resulting in brittle fracture, poor plasticity, and low strength [3–5]. Therefore, in the production process, the alloy needs to be modified to change the coarse needle flake eutectic silicon into fine fibrous, to improve the strength and plasticity of the alloy [6–8].

Before casting, it is necessary to quickly and accurately evaluate the effect of melt modification [9]. The metallographic observation method is the most intuitive evaluation method for the modification effect, but it is not suitable for rapid evaluation in front of the furnace because of its long operation period. The chemical analysis method evaluates the modification effect by detecting the content of modifiers in the melt, which has the advantage of fast detection speed. However, the modification effect is related not only to the content of the modifier but also to treatment time, cooling conditions, and effective time [10, 11]. Therefore, it is difficult to evaluate the modification effect only by chemical composition accurately. Thermal analysis has attracted the attention of experts and

*Corresponding author: e-mail address: hlgchxy06318@163.com

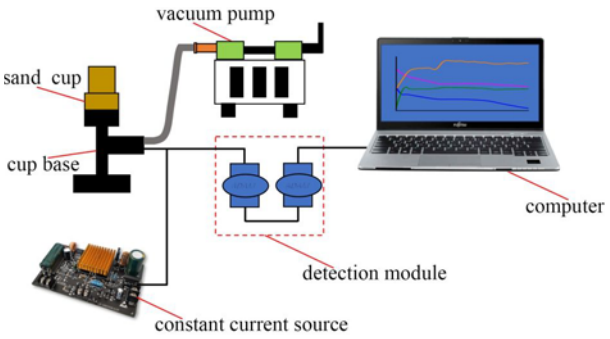

Fig. 1. Overall composition diagram of melt resistivity monitoring device.

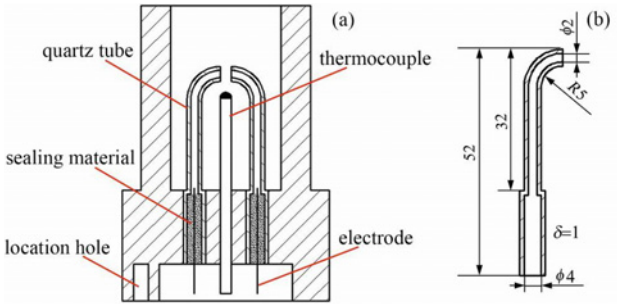

Fig. 2. Sample cup structure and quartz tube size drawing: (a) sample cup structure, (b) quartz tube size.

scholars due to its advantages of convenience, economy, and efficiency [12, 13], among which the change of eutectic growth temperature before and after modification is the most widely used to evaluate the modification effect [14–16]. Resistivity is a sensitive parameter of alloy structure, which can characterize the change of alloy melt structure and the formation of a new phase during alloy solidification [18]. In the case of given technological conditions, the resistivity is related to the composition and relative content of the alloy and the microstructure [19, 20]. Thermal analysis taking phase transition heat as its characteristic value and resistivity method taking conductivity change as its characteristic value are the two methods to monitor the microstructure change of melt solidification process from different perspectives. The thermal analysis method has a long history of research and application and is relatively mature, while the resistivity method is only limited to the experimental research stage under laboratory conditions [21–23]. To realize the application of the resistivity method in real production and expand it to the evaluation of alloy modification effect in front of the furnace, a modification effect evaluation system of hypoeutectic Al-Si alloy for practical production is designed in this paper. Based on this system, an experimental study on the relationship between resistivity change and modification effect during the melt solidification process was carried out, and a simple model for rapidly evaluating the modification effect was established.

2. Alloy melt resistivity monitoring device

2.1. General structure of the device

The general structure of the alloy melt resistivity monitoring device is shown in Fig. 1, including a sample cup, sample cup base support, vacuum aspiration unit, constant current power supply, data acquisition module, and computer. The resistivity of alloy melt is measured by the two-electrode method. The constant power supply supplies a constant current to the alloy melt in the quartz tube through the electrodes at the lower end of the quartz tube. The data acquisition module obtains the voltage signal through the electrodes. The sample cup base support is equipped with a constant current power supply, negative pressure air source access, and a thermocouple signal export device. The data acquisition module ADAM4118 is connected to the computer, and the data acquisition program is written in the Visual Basic language. After the melt is poured into the sample cup, the data acquisition program automatically monitors the melt surface position in the cup according to the thermocouple temperature and timely starts the vacuum aspiration unit and constant current power supply to ensure that the melt is sucked into the L-shaped double tube conductivity cell and forms a closed-loop loop. The resistivity channel of the data acquisition module will monitor the resistivity change of the conductivity cell in real time. Because the melt in the conductivity cell solidifies synchronously with the melt in the cup, the solidification behavior of the melt inside and outside the conductivity cell can be considered basically synchronous and consistent.

2.2. Sample cup structure

The structure of the sample cup is shown in Fig. 2a. The sample cup is made of resin sand, the inner cavity is cylindrical, the temperature measuring point of the thermocouple is placed at the geometric center of the inner cavity, L-shaped quartz tubes are installed on both sides of the thermocouple to form a U-shaped conductivity cell, and the lower end of the quartz tube is sealed with sealing material to prevent the passage of aluminum alloy melt. The specific size of the quartz tube is shown in Fig. 2b.

The resistance value of the material is directly proportional to the length and inversely proportional to the cross-sectional area. If the spatial structure of the sample cup allows, the longer the conductivity cell length and the thinner the inner diameter are, the

Table 1. Chemical composition of ZL101A alloy with different Sr addition level

Sr addition level (mass%)	Element (mass%)							
	Si	Sr	Mg	Zn	Fe	Mn	Ti	Al
0	7.06	0	0.32	0.012	0.98	0.012	0.152	Bal.
0.01	7.09	0.009	0.31	0.009	0.97	0.011	0.192	Bal.
0.02	6.98	0.021	0.32	0.011	0.98	0.010	0.152	Bal.
0.03	6.99	0.029	0.31	0.015	0.96	0.009	0.155	Bal.
0.04	7.02	0.041	0.31	0.008	0.91	0.011	0.150	Bal.
0.05	6.98	0.050	0.32	0.013	0.95	0.013	0.151	Bal.

better the resistivity parameter monitoring is, and the obtained parameters can more sensitively reflect the changes in material microstructure. Under the condition of limited sample cup space, two quartz tubes with an inner diameter of 2 mm are used as the conductivity cell. The purpose of designing the quartz tube into an L-shape is to increase the length of the conductivity cell. To ensure the accuracy of resistivity measurement, the geometric parameters of quartz tubes were calibrated using high-purity mercury (99.99 mass%) with known resistivity at room temperature.

3. Resistivity monitoring test during melt solidification

3.1. Alloy melting and modification treatment

ZL101A commercial hypoeutectic Al-Si alloy was selected as the test material. In each experiment, 1 kg ZL101A alloy was melted in a crucible resistance furnace at 720 ± 5 ℃. The alloy melt was degassed under high purity argon gas for 15 min and then added to Al-10Sr master alloy. After adding the modifier, the alloy melt was maintained for 30 min and then poured into a resin sand sample cup. The addition levels of Sr were 0, 0.01 mass%, 0.02 mass%, 0.03 mass%, 0.04 mass%, and 0.05 mass%. The chemical composition of the original ZL101A alloy and the alloy added with Sr was determined by a direct-reading spectrometer. The results are shown in Table 1. The temperature and resistivity changes of the alloy from liquid to solid were recorded. The samples were taken from the solidified alloy near the tip of the thermocouple. After grinding and polishing by standard procedures, they were corroded with 0.5 % hydrofluoric acid aqueous solution for 10 to 15 s. Then the microstructure was observed by scanning electron microscope, and the size of eutectic silicon was counted by Image-Pro software. Twenty fields of view were selected for the alloy microstructure with each Sr addition level, and the perimeters of all eutectic silicon in each field were measured. The ML (modification effect) was determined by using the following formula [16]:

$$\mathrm{ML} = (1 \times a\%) + (2 \times b\%) + (3 \times c\%) + (4 \times d\%) + (5 \times e\%) + (6 \times f\%), \quad (1)$$

where $a\%$–$f\%$ are percentages for Classes 1–6, respectively.

3.2. Influence of the addition level of Sr modifier on the resistivity of melt

Figure 3 shows the curves of temperature and resistivity with time for different Sr addition levels. Before the eutectic reaction, the resistivity decreases with the drop in temperature. After the eutectic reaction begins, the shape of the resistivity curve is similar to the cooling curve, the curve rises first, and then a plateau appears. The position of the plateau slightly lags behind the eutectic temperature plateau. After the plateau appears for a short time, the resistivity declines. The first derivative curves of temperature and resistivity curves are made to obtain the relevant characteristic values on the curves. There is a plateau on the cooling curve at the eutectic growth stage, and the plateau value is the eutectic growth temperature T_{EG}. There is also a plateau on the resistivity curve at this stage, and the plateau value is defined as ρ_{EG}. The T_{EG} value is the temperature value corresponding to the eutectic stage when the $\mathrm{d}T/\mathrm{d}t$ value is zero, and the ρ_{EG} value is the resistivity value when the $\mathrm{d}\rho/\mathrm{d}t$ value is zero in the eutectic stage. At the same time, the first derivative of temperature is used to calculate the cooling rates of the alloys with different Sr addition levels. The cooling rates of the alloys with 0 to 0.05 mass% Sr addition levels are 1.268, 1.257, 1.269, 1.272, 1.254, and 1.259 ℃ s^{-1}, respectively. The cooling rates are very close, and the alloy melts with different Sr addition levels can be considered to solidify under the same cooling condition.

Figure 4 shows the cooling curves of the alloys with different Sr addition levels at the eutectic stage. It is evident that the plateau on the cooling curves at the eutectic stage presents a downward trend with the increase of Sr addition levels. The T_{EG} value of the alloy

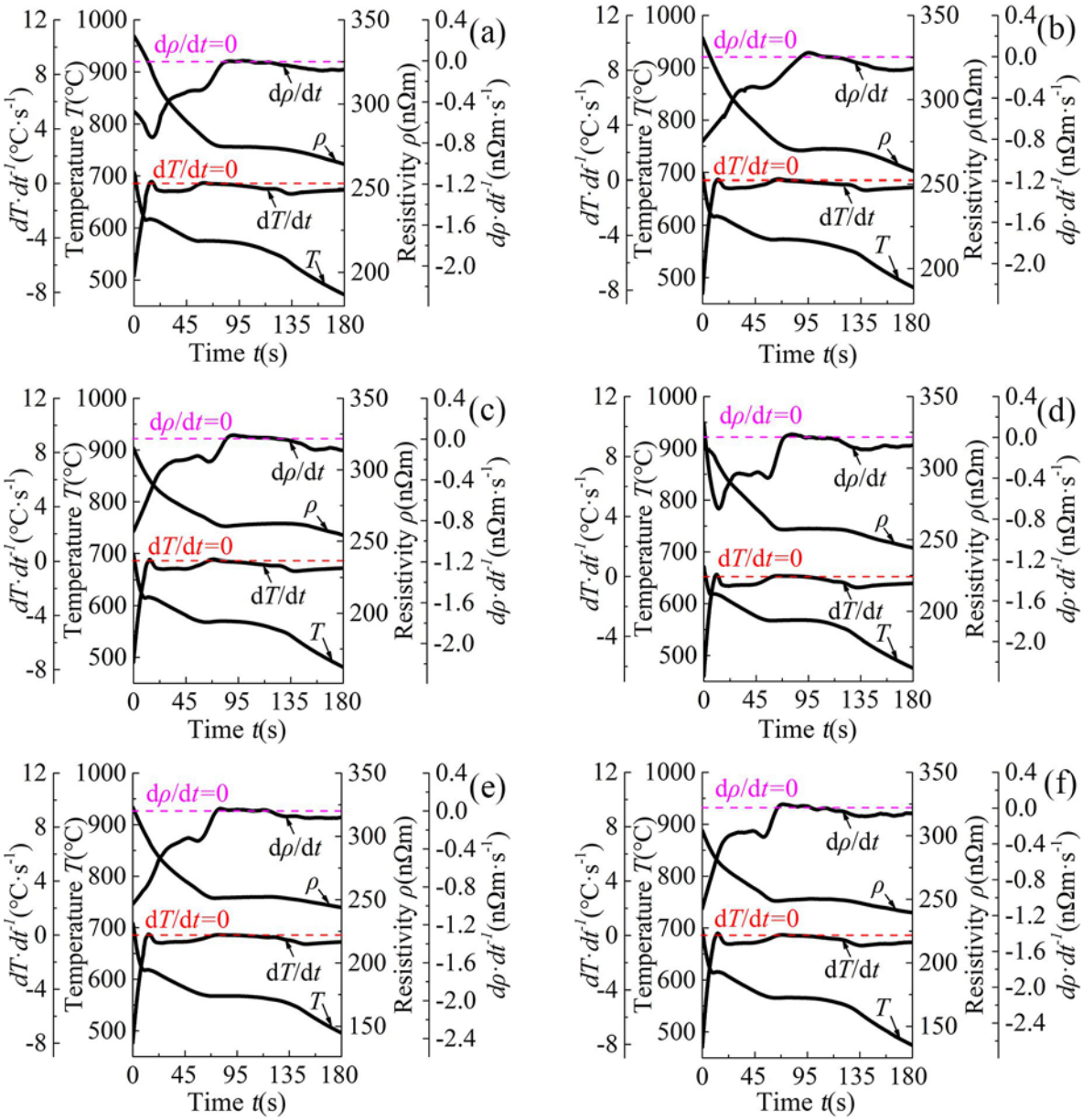

Fig. 3. The curves of temperature and resistivity with time for different Sr addition levels: (a) 0 Sr, (b) 0.01 mass% Sr, (c) 0.02 mass% Sr, (d) 0.03 mass% Sr, (e) 0.04 mass% Sr, and (f) 0.05 mass% Sr.

without Sr addition is 575.4 ℃, and the T_{EG} values of the alloys with Sr addition levels of 0.01 mass% to 0.05 mass% are 573.5, 570.0, 568.5, 567.6, and 566.2 ℃, respectively. The characteristic value ΔT_{EG}, which is the difference value of the eutectic growth temperature of the alloy before and after modification, is generally used to evaluate the modification effect of Al-Si alloy by thermal analysis. The ΔT_{EG} values of the alloys with 0.01 mass% Sr to 0.05 mass% Sr are 1.9, 5.4, 6.9, 7.8, and 9.2 ℃, respectively.

Figure 5 shows the resistivity curves of the alloys with different Sr addition levels at the eutectic stage. It is evident that the plateau on the resistivity curves at the eutectic stage presents a downward trend with the increase of Sr addition levels. The ρ_{EG} value of alloy without Sr addition is 274.4 nΩ m, and the ρ_{EG} values of alloys with Sr addition levels of 0.01 mass% to 0.05 mass% are 270.7, 262.4, 257.7, 252.1, and 250.1 nΩ m, respectively. By analogy with ΔT_{EG}, we defined $\Delta\rho_{EG}$, which is the difference value of the plateau value of the resistivity curve of the alloy before and after modification. The $\Delta\rho_{EG}$ values of the alloys with 0.01 mass% Sr to 0.05 mass% Sr are 3.7, 12.0, 16.7, 22.3, and 24.3 nΩ m, respectively.

During the solidification of hypoeutectic Al-Si alloys, the primary α-Al phase precipitates at first and releases a large amount of latent heat. When the rate of releasing latent heat is equivalent to the rate of cool-

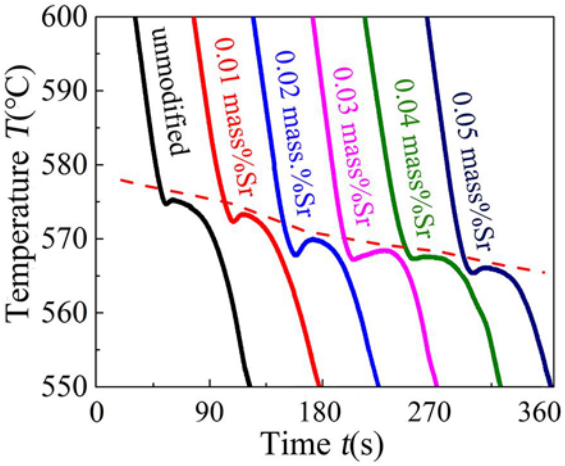

Fig. 4. The temperature with time curves of the alloys with different Sr addition levels.

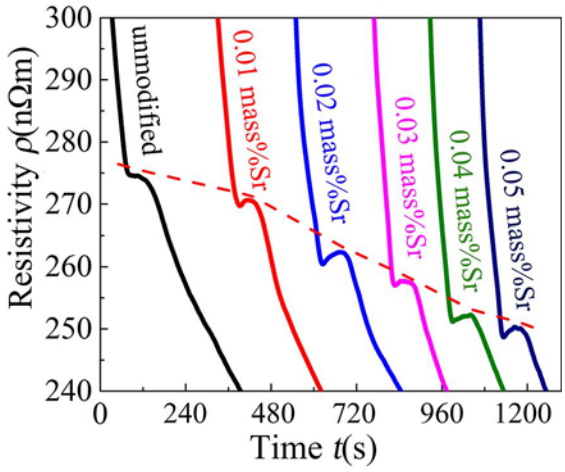

Fig. 5. The resistivity with time curves of the alloys with different Sr addition levels.

ing heat loss, a primary crystal plateau will appear on the cooling curve. At the late solidification stage of the primary crystal phase, the growth of primary α-Al is slow, and the latent heat released is less, leading to a continuous temperature drop. When the temperature drops to the eutectic point, the eutectic reaction begins to occur, and the eutectic β-Si phase and eutectic α-Al phase are precipitated, which will also release a large amount of latent heat. When the heat release rate is equivalent to the heat loss rate, a eutectic plateau will appear on the cooling curve. Figure 6 shows the relationship between the solidification process at the eutectic stage and the cooling curve and resistivity curve changes. The relationship between the eutectic stage solidification process of Al-Si alloy and temperature change has been studied by scholars [24]. When the temperature drops to the eutectic point,

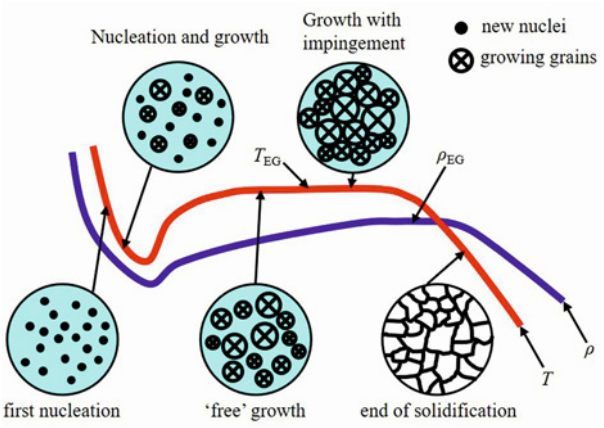

Fig. 6. The relationship between the solidification process at the eutectic stage and the cooling curve and resistivity curve changes.

the eutectic phases begin to nucleate and release latent heat, the cooling rate of the alloy slows down, the subsequent crystal nuclei begin to grow, and new crystal nuclei are generated. With the generation and growth of a large number of crystal nuclei, the rate of releasing latent heat exceeds the rate of cooling heat loss of the alloy, which makes the cooling curve of the alloy show an upward trend. After the nucleation of the alloy is completed, the crystal nucleus begins to grow freely. With the rapid growth of the crystal nucleus, a large number of crystal nucleus edges begin to contact. When the release rate of latent heat is equivalent to the rate of heat loss, a eutectic plateau will be generated on the cooling curve. At the later stage of eutectic solidification, as the growth rate of the eutectic structure slows down, the release rate of latent heat is less than the rate of heat loss, and the cooling curve begins to decline. When all eutectic nuclei grow to complete contact with adjacent nuclei, the growth stops, and solidification ends.

In the eutectic reaction, the eutectic β-Si phase and eutectic α-Al phase are precipitated, and eutectic β-Si grows ahead of the eutectic α-Al phase. After the eutectic reaction starts, the precipitation of the eutectic β-Si phase has high resistivity, which has a great scattering effect on electrons, and shows an effect of the increase in resistivity. At the same time, the release of the latent heat of the eutectic reaction increases the temperature, which enhances the disturbance to the alloy melt and the scattering of free electrons, so it shows an effect of the increase on resistivity. Therefore, the overall resistivity of the alloy melt shows an upward trend under the influence of temperature and the eutectic β-Si phase. The electric conductivity of eutectic α-Al phase particles is better than that of the surrounding melt. When the free electrons collide with the eutectic α-Al phase particles, they will not be scattered but pass through.

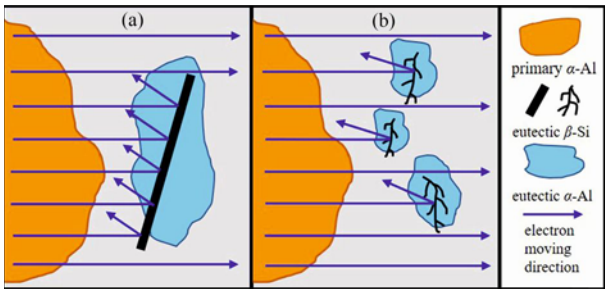

Fig. 7. The effects on the passage of free electrons of different forms of eutectic β-Si phase: (a) without modification and (b) after modification.

Moreover, the collision probability of the free electrons inside the eutectic α-Al phase particles is less than that of the melt, which increases the average free path of the free electrons. Therefore, the eutectic α-Al phase shows an effect of a decrease in resistivity. At the later stage of eutectic solidification, the growth rate of the eutectic α-Al phase gradually catches up with the eutectic β-Si phase. At the same time, the temperature in the later stage of the eutectic reaction begins to drop, which weakens the disturbance to the alloy melt, and reduces the scattering of free electrons, so it shows an effect of a decrease in resistivity. Because the resistivity of the alloy is mainly affected by temperature, the type and size of phases in the alloy [25], it is possible to achieve a balance for the effects

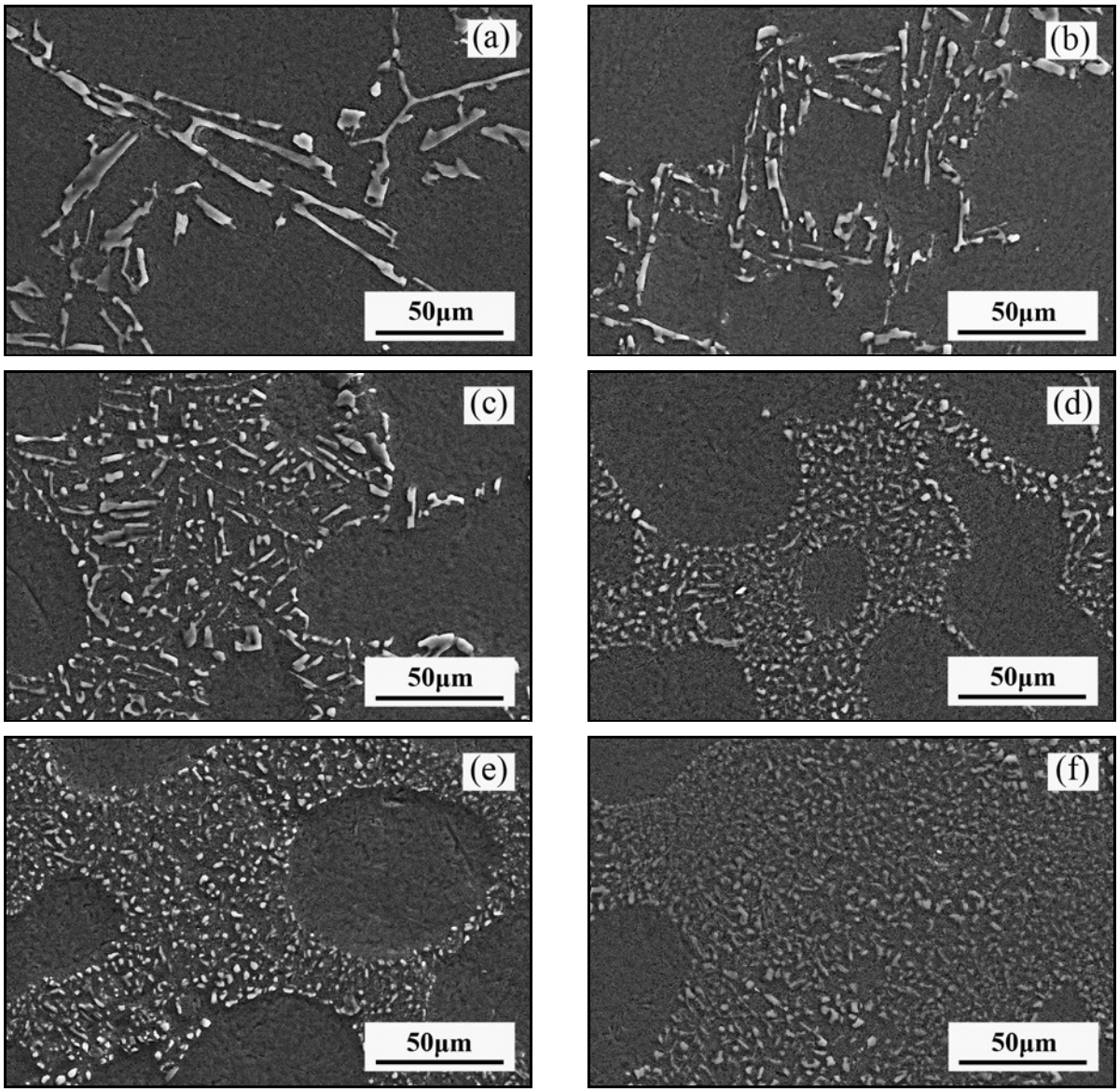

Fig. 8. The microstructure of the alloys with different Sr addition levels: (a) 0 Sr, (b) 0.01 mass% Sr, (c) 0.02 mass% Sr, (d) 0.03 mass% Sr, (e) 0.04 mass% Sr, and (f) 0.05 mass% Sr.

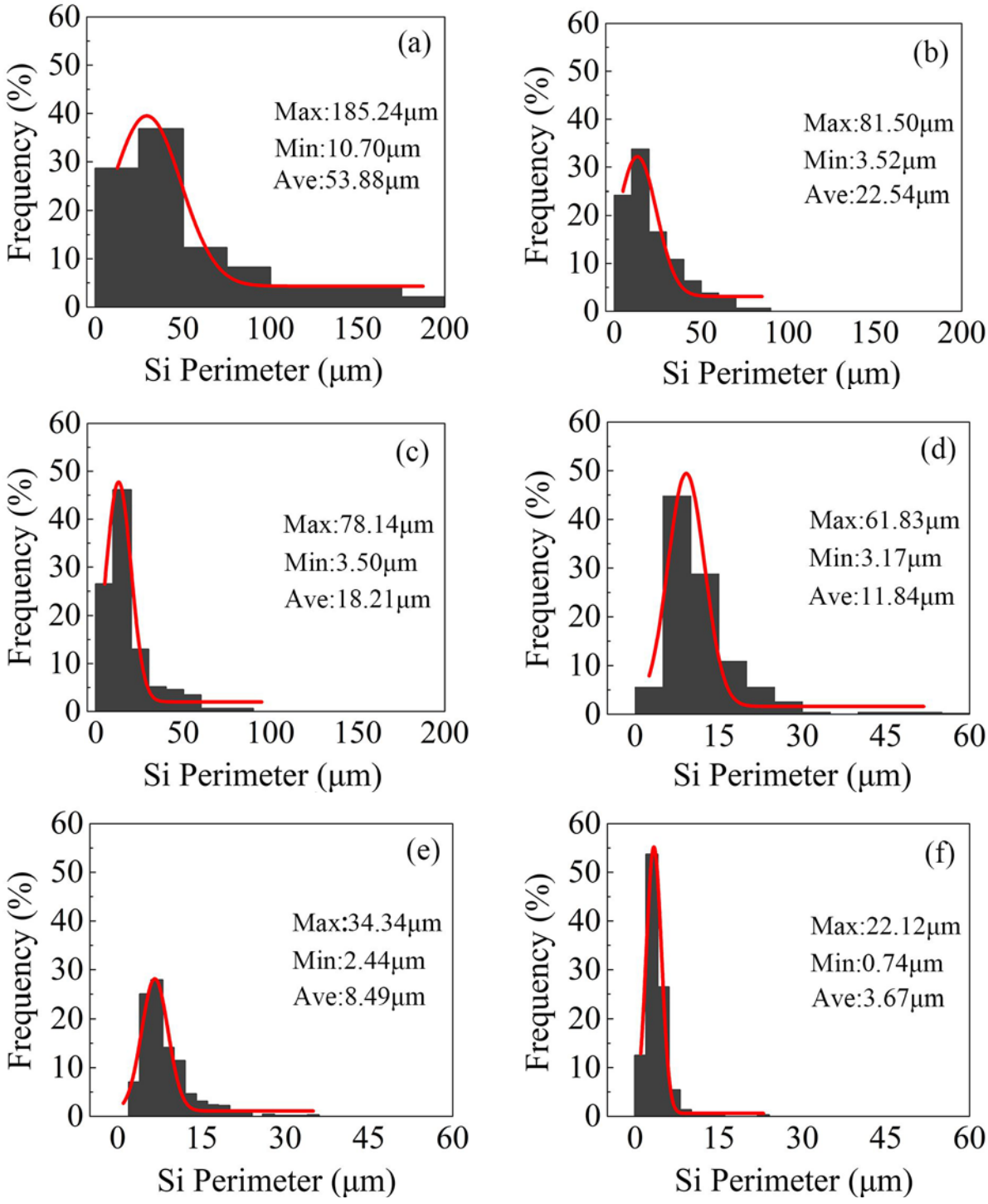

Fig. 9. The perimeter distribution of eutectic silicon: (a) 0 Sr, (b) 0.01 mass% Sr, (c) 0.02 mass% Sr, (d) 0.03 mass% Sr, (e) 0.04 mass% Sr, and (f) 0.05 mass% Sr.

of the eutectic β-Si phase, eutectic α-Al phase, and temperature on resistivity, and a plateau will appear on the resistivity curve. After that, with the end of the eutectic reaction and the alloy completely solidified, temperature becomes the main factor affecting the resistivity. With the further decrease in temperature, the resistivity shows a downward trend.

Sr modifier inhibits the nucleation and growth of eutectic phases, so the eutectic temperature plateau decreases. At the same time, the Sr modifier will change the original growth mode of eutectic β-Si, and make the coarse plate-like eutectic β-Si phase change to fine fibrous. Therefore, a finer eutectic β-Si structure is obtained after modification. The size of the

eutectic β-Si phase greatly influences the conductivity of alloy melt. Figure 13 shows the effects on the passage of free electrons of different forms eutectic β-Si phase [26]. For Al-Si alloy without modification, the microstructure of the eutectic β-Si phase is coarse plate-like or long needle. As shown in Fig. 7a, this can effectively increase the probability of collision between the eutectic β-Si phase and free electrons, which is not conducive to the smooth passage of electrons. Thus, it has a great effect on increasing the resistivity of alloy melt. After modification, the eutectic β-Si phase presents as fine fibrous, which reduces the probability of collision with free electrons and increases the probability of electrons passing through (Fig. 7b). Compared with the alloy without modification, the physical properties of the alloy show lower resistivity. After Sr modification, the eutectic growth temperature of the alloy decreases, and the eutectic β-Si particles become fine, which will make the improved strength of the resistivity after the precipitation of the eutectic β-Si phase less than that of unmodified alloy. Therefore, the effects of the eutectic β-Si phase, eutectic α-Al phase, and temperature on the resistivity of the modified alloy melt will be balanced at a lower resistivity level. It shows that the resistivity plateau with the time curve moves downward, and the ρ_{EG} value becomes smaller.

3.3. Relationship between resistivity and modification level during melt solidification

The microstructure of the alloys with different Sr addition levels is shown in Fig. 8. It can be seen from Fig. 3a that the eutectic silicon phase is coarse lamellar or acicular shape when it is not modified. When the Sr addition level is 0.01 mass%, as shown in Fig. 8b, the length of needle sheet shape eutectic silicon became shorter and tended to change to a fibrous shape. As shown in Fig. 3c, when the addition level of Sr is 0.02 mass%, the morphology of eutectic silicon has changed to a fibrous shape, and the size of eutectic silicon is further reduced, but most eutectic silicon is short needle flake shape. When the addition level of Sr increases to 0.03 mass%, as shown in Fig. 8d, the morphology of eutectic silicon changes into a fibrous shape, most of the eutectic is spot-like, but there are a small number of eutectic silicon particles with slightly longer size. When the Sr addition level is 0.04 mass%, it can be seen from Fig. 8e that almost all eutectic silicon is distributed spot-like, and the number of small-size eutectic silicon increases. As shown in Fig. 8f, when the Sr addition level is 0.05 mass%, many smaller spot-like eutectic silicon particles appear, and the number of small-size eutectic silicon further increases. With the increase of the Sr addition level, the effect of improving the microstructure of the alloy gradually becomes stronger.

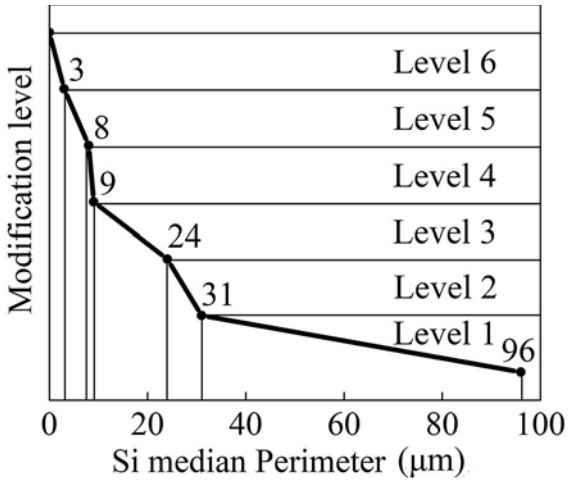

Fig. 10. The median value of the perimeter at each modification level was used to define the upper limits of this parameter for the corresponding modification levels.

The perimeter distribution of eutectic silicon of the alloys with different Sr addition levels is shown in Fig. 9. It can be seen that the perimeter distribution of eutectic silicon before and after modification basically followed the normal distribution, the size distribution of unmodified eutectic silicon is relatively scattered, there is a large proportion of large-size eutectic silicon, and the size distribution of eutectic silicon after modification is relatively concentrated. With the increase of the Sr addition level, the amount of large-size eutectic silicon decreases gradually, while the proportion of small-size eutectic silicon increases gradually. The average perimeter of the eutectic silicon of unmodified alloy is 53.88 μm. When Sr addition level is 0.05 mass%, the average perimeter of eutectic silicon decreases to 3.67 μm, indicating that the size of eutectic silicon could be significantly reduced after adding Sr.

M. Djurdjevic et al. [16] statistically calculated the size of eutectic silicon in the standard chart in Al-Si casting of the American Foundry Association and found that there was a good corresponding relationship between the perimeter of eutectic silicon and the modification level. In their work, the median perimeter was used to define the upper limits of the perimeter parameter for each modification level. For example, the median perimeter at modification level 6 is 3 μm, so a silicon structure with a perimeter less than 3 μm is treated as modification level 6, as shown in Fig. 10. Based on Fig. 10, we calculate the percentage of eutectic silicon structure of the alloys with different Sr addition levels in different modification levels, as shown in Table 2. Then, according to Eq. (1), the modification levels of the alloys with different Sr addition levels are rated, as shown in Fig. 11. It is evident that the modification level increases with

Table 2. The percentage of eutectic silicon particles in different modification levels in alloys with different Sr addition levels

Sr addition level (mass%)	Fractions (%)					
	Level 1	Level 2	Level 3	Level 4	Level 5	Level 6
	63.26	8.16	28.58	0.00	0.00	0.00
0.01	25.47	10.19	43.95	5.09	15.30	0.00
0.02	14.04	5.06	63.48	2.81	14.61	0.00
0.03	1.71	3.62	54.37	8.32	31.98	0.00
0.04	0.51	0.51	31.77	7.47	58.61	1.11
0.05	0.00	0.00	1.50	0.64	57.30	40.56

Table 3. The modification levels and the characteristic values of temperature and resistivity of alloys with different Sr addition levels

Sr addition level (mass%)	T_{EG} (℃)	ΔT_{EG} (℃)	ρ_{EG} (nΩ m)	$\Delta\rho_{EG}$ (nΩ m)	ML
0	575.4	0	274.4	0	1.65
0.01	573.5	1.9	270.7	3.7	2.75
0.02	570.0	5.4	262.4	12.0	3.00
0.03	568.5	6.9	257.7	16.7	3.65
0.04	567.6	7.8	252.1	22.3	4.26
0.05	566.2	9.2	250.1	24.3	5.37

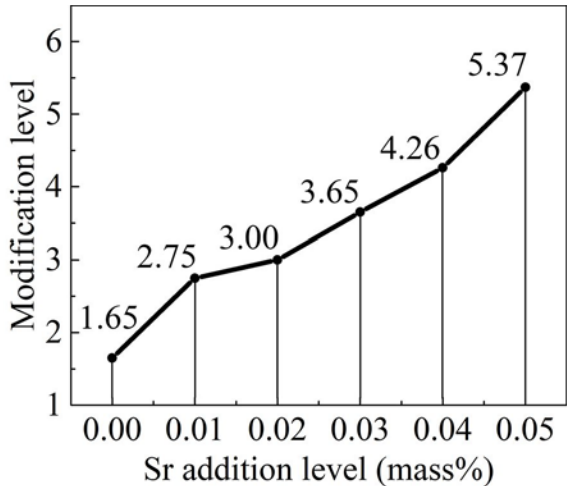

Fig. 11. The modification levels of the alloys with different Sr addition levels.

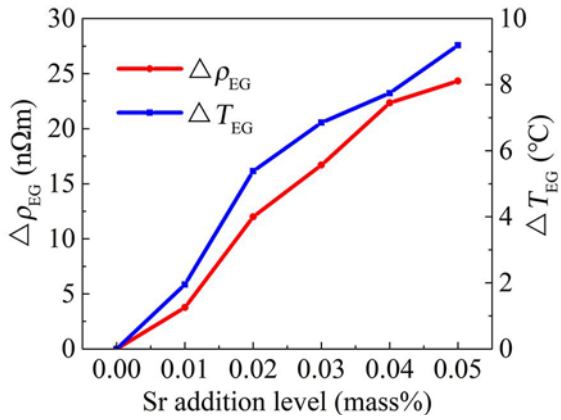

Fig. 12. The relationship between Sr addition levels and $\Delta\rho_{EG}$ and ΔT_{EG}.

the increase of the Sr addition level. And when the Sr addition level is 0.05 mass%, the modification level reaches class 5.37.

The modification levels and the characteristic values of temperature and resistivity of alloys with different Sr addition levels are shown in Table 3. The changes of ΔT_{EG} and $\Delta\rho_{EG}$ with the addition level of Sr are shown in Fig. 12. It can be seen from the figure that ΔT_{EG} and $\Delta\rho_{EG}$ increase with the increase of the Sr addition level. ΔT_{EG}, $\Delta\rho_{EG}$, and modification level are related to the addition level of Sr, so ΔT_{EG} and $\Delta\rho_{EG}$ are strongly correlated with modification level. Figure 13 shows the relationship between $\Delta\rho_{EG}$ and modification level. It can be seen that the modification level increases with the increase of $\Delta\rho_{EG}$. The relationship between them is fitted, and the evaluation model of the modification level of hypoeutectic Al-Si alloy is established as follows:

$$\mathrm{ML} = 1.68089 + 0.36432\Delta\rho_{EG} - 0.03043\Delta\rho_{EG}^2 + 8.83689 \times 10^{-4}\Delta\rho_{EG}^3. \quad (2)$$

Its correlation coefficient $R^2 = 0.97887$, close to 1, proving that the fitting effect is good.

To verify the accuracy of the model, the modification effect of five groups of alloys with different Sr ad-

Table 4. The modification levels obtained by the mathematical model and the modification method

Sr addition level (mass%)	$\Delta\rho_{EG}$ (nΩ m)	Resistivity method ML	Metallographic method ML	Difference
0.015	2.5	2.42	2.95	0.53
0.025	8.7	3.13	3.35	0.22
0.035	21.4	4.20	3.93	0.27
0.045	23.3	4.83	4.76	0.07
0.055	25.6	5.89	5.88	0.01

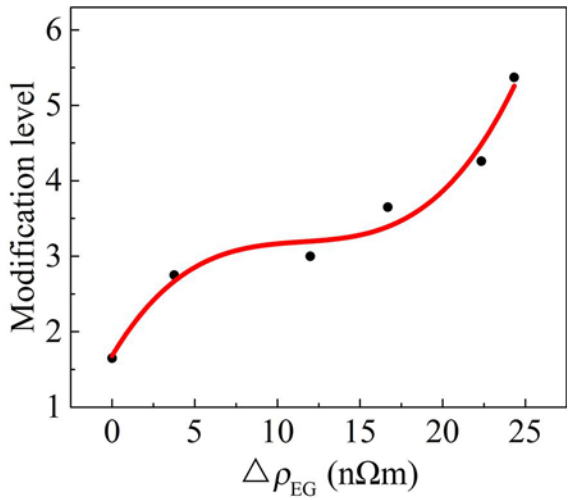

Fig. 13. The relationship between modification levels and $\Delta\rho_{EG}$.

dition levels is evaluated. The modification levels obtained by the mathematical model are compared with those obtained by the metallographic method. The addition levels of Sr in the verification test, the modification levels obtained by the mathematical model, and the modification levels obtained by the metallographic method are shown in Table 4. It can be seen from Table 4 that the modification levels obtained by the resistivity method are very close to those obtained by the metallographic method. And in 4 of the 5 tests, the difference in modification level is less than 0.5. When the modification level error is within ± 0.5, the accuracy is up to 80 %.

4. Discussion

Resistivity is a sensitive physical property parameter of alloy structure and plays an important role in analyzing alloy melt and solid alloy structures [18–20]. The resistivity can reflect electron transport properties, and the microstructure evolution information of alloy can be obtained from a more microscopic perspective [25]. The resistivity of alloy melt is mainly affected by temperature, phase type, and phase size. The change of $\Delta\rho_{EG}$ is mainly affected by the change in eutectic structure nucleation, growth temperature, and the size of eutectic silicon particles. Therefore, the resistivity evaluation will reflect whether eutectic silicon is refined after modification. Thermal analysis can indirectly obtain the degree of refinement of eutectic silicon by monitoring the changes in eutectic structure nucleation and growth temperature caused by a modifier. But sometimes, although some modifiers cause the change of eutectic structure nucleation and growth temperature, the modification effect is not good [14]. Therefore, the resistivity method is more direct than the thermal analysis method.

The designed melt resistivity monitoring system has the advantages of convenient operation and overcomes the disadvantages of complex operation and the demanding operation environment of existing resistivity monitoring equipment. The modification effect evaluation of hypoeutectic Al-Si alloy can be completed within 3 min, and the detection speed is fast. There is a strong correlation between $\Delta\rho_{EG}$ and modification level, and the correlation coefficient $R^2 = 0.97887$, close to 1. The model was verified by experiments, and the accuracy reached 80 % when the modification level error was within ± 0.5. The rapid evaluation test of aluminum alloy melt modification effect based on melt resistivity is preliminary, and it is expected that there will be an extensive research space in the following aspects:

(1) The structure of the sample cup and conductivity cell is optimized to make the alloy melt fill the conductivity cell without the vacuum aspiration device, which will greatly simplify the overall structure of the monitoring system.

(2) By changing the relative position of the electrode flexibly, the solidification microstructure of different locations can be evaluated so that the modification effect of alloy can be evaluated comprehensively and accurately.

(3) Mining the relevant characteristic values and refining the evaluation model with more characteristic values will help to improve further the accuracy of the evaluation of the modification effect.

(4) The modification effect of the alloy is mainly affected by nucleation and growth. The thermal analysis method has advantages over the resistivity method in monitoring the nucleation changes and growth temperature of the eutectic structure, while the resistiv-

ity method has advantages over the thermal analysis method in monitoring the actual eutectic silicon particle refinement. The combination of resistivity and thermal analysis can be used further to analyze the nucleation and growth process of the eutectic structure and play a more significant role in the evaluation of the modification effect.

5. Conclusions

(1) In this paper, a resistivity monitoring system is constructed for the aluminum alloy melt solidification process. The system consists of a sample cup, sample cup base support, vacuum aspiration unit, constant current power supply, data acquisition module, and computer. The evaluation of the modification effect can be completed within 3 minutes by using the system to realize the rapid evaluation of the modification effect of the aluminum alloy melt in front of the furnace under production conditions.

(2) Through the electrical resistivity monitoring test of hypoeutectic Al-Si alloy with different modification effects, it is found that the plateau value ρ_{EG} of resistivity curve with time in eutectic stage decreases, and the difference $\Delta\rho_{EG}$ of plateau value ρ_{EG} before and after modification increases with the increase of modification level. Thus, the evaluation model of the modification of hypoeutectic Al-Si alloy is established. The evaluation model can be expressed as: $ML = 1.68089 + 0.36432\Delta\rho_{EG} - 0.03043\Delta\rho_{EG}^2 + 8.83689 \times 10^{-4}\Delta\rho_{EG}^3$ (the correlation coefficient $R^2 = 0.97887$).

(3) The experimental results in this paper prove that the rapid evaluation method of aluminum alloy melt modification effect in front of the furnace based on melt resistivity has application prospects. Meanwhile, there is a large space for further research, which is worthy of further discussion in sampling method improvement, conductivity cell structure optimization, evaluation model research, and combined application with the thermal analysis method.

References

[1] D. Jiang, J. Yu, Simultaneous refinement and modification of the eutectic Si in hypoeutectic Al-Si alloys achieved via the addition of SiC nanoparticles, J. Mater. Res. Technol. 8 (2019) 2930–2943. https://doi.org/10.1016/j.jmrt.2019.05.001

[2] B. Akyuz, Effect of Si content on machinability of Al-Si alloys, Kovove Mater. 55 (2017) 237–244. https://doi.org/10.4149/km_2017_4_237

[3] J. Chen, C. Liu, F. Wen, Q. Zhou, H. J. Zhao, R. G. Guan, Effect of microalloying and tensile deformation on the internal structures of eutectic Si phase in Al-Si alloy, J Mater. Res. Technol. 9 (2020) 4682–4691. https://doi.org/10.1016/j.jmrt.2020.02.096

[4] R. Aparicio, C. Gonzalez-Rivera, M. Ramirez-Argaez, G. Barrera, G. Trapaga, Newton thermal analysis of unmodified and strontium modified Al-Si alloys. Kovove Mater. 51 (2013) 211–220. https://doi.org/10.4149/km_2013_4_211

[5] M. De-Giovanni, A. J. Kaduk, P. Srirangam, Modification of Al-Si alloys by Ce or Ce with Sr, JOM 71 (2019) 426–434. https://doi.org/10.1007/s11837-018-3192-6

[6] Q. Zheng, L. Zhang, H. Jiang, J. Zhao, J. He, Effect mechanisms of micro-alloying element La on microstructure and mechanical properties of hypoeutectic Al-Si alloys, J. Mater. Sci. Technol. 47 (2020) 142–151. https://doi.org/10.1016/j.jmst.2019.12.021

[7] W. Wang, Y. Liu, J. Zhu, Y. Liu, X. Su, Effect of complex modification on microstructure and mechanical properties of hypoeutectic Al-Si, Metallogr. Microstruc. 8 (2019) 833–839. https://doi.org/10.1007/s13632-019-00584-7

[8] H. M. Lus, Effect of casting parameters on the microstructure and mechanical properties of squeeze cast A380 aluminum die cast alloy, Kovove Mater. 50 (2013) 243–250. https://doi.org/10.4149/km_2012_4_243

[9] D. Q. Shi, D. Y. Li, G. L. Gao, L. H. Wang, Experimental study on new method and automatic system for fast evaluating Al-Si alloy modification effect in front of furnace, Sci. China Ser. E. 49 (2006) 569–575. https://doi.org/10.1007/s11431-006-2003-4

[10] B. Li, H. Wang, J. Jie, Z. Wei, Microstructure evolution and modification mechanism of the ytterbium modified Al-7.5%Si-0.45%Mg alloys, J. Alloy Compd. 509 (2011) 3387–392. https://doi.org/10.1016/j.jallcom.2010.12.081

[11] G. L. Zhu, N. J. Gu, B. J. Zhou, Effects of combining Na and Sr additions on eutectic modification in Al-Si alloy, IOP Conference Series: Materials Science and Engineering 230 (2017) 012015. https://doi.org/10.1088/1757-899X/230/1/012015

[12] N. Jamaly, N. Haghdadi, A. B. Phillion, Microstructure, macrosegregation, and thermal analysis of direct chill cast AA5182 aluminum alloy, J. Mater. Eng. Perform. 24 (2015) 2067–2073. https://doi.org/10.1007/s11665-015-1480-7

[13] N. Haghdadi, A. B. Phillion, D. M. Maijer, Microstructure characterization and thermal analysis of aluminum alloy B206 during solidification, Metall. Mater. Trans. A 46 (2015) 2073–2081. https://doi.org/10.1007/s11661-015-2780-0

[14] S. S. Wu, M. J. Lv, J. X. Chen, Y. W. Mao, S. L. Lv, Effects of Sb on Al7SiMg alloy measured with cooling curve analysis, Mater. Sci. Forum 879 (2017) 2113–2118. https://doi.org/10.4028/www.scientific.net/MSF.879.2113

[15] M. Malekan, S. G. Shabestari, Computer-aided cooling curve thermal analysis used to predict the quality of aluminum alloys, J. Therm. Anal. Calorim. 103 (2010) 453–458. https://doi.org/10.1007/s10973-010-1023-2

[16] M. Djurdjevic, H. Jiang, J. Sokolowski, On-line prediction of aluminum-silicon eutectic modification level using thermal analysis, Mater. Charact. 46 (2001) 31–38. https://doi.org/10.1016/S1044-5803(00)00090-5

[17] M. Mahfoud, A. K. Prasada Rao, D. Emadi, The role of thermal analysis in detecting impurity levels during aluminum recycling, J. Therm. Anal. Calorim. 100

(2010) 847–851.
https://doi.org/10.1007/s10973-010-0742-8
[18] I. Stulikova, J. Faltus, B. Smola, Influence of composition on natural ageing of Al-Mg-Si alloys, Kovove Mater. 45 (2007) 85–90.
[19] D. D. Yang, F. Q. Zu, X. Y. Li, X. Cui, X. Lv, L. Li, On electrical resistivity evolution of Sn-Sb10 melt during isothermal processes at different temperatures, Phys. Chem. Liq. 49 (2011) 648–654. https://doi.org/10.1080/00319104.2010.492472
[20] S. Zhou, C. H. Yang, S. K. Lin, A. N. Al Hazaa, O. Mokhtari, X. Liu, and H. Nishikawa, Effects of Ti addition on the microstructure, mechanical properties and electrical resistivity of eutectic Sn58Bi alloy, Mater. Sci. Eng. A 744 (2019) 560–569.
https://doi.org/10.1016/j.msea.2018.12.012
[21] Y. Sun, H. Muta, K. Kurosaki, Y. Ohishi, Thermal and electrical conductivity of liquid Al-Si alloys, Int. J. Thermophys. 40 (2019) 1–10.
https://doi.org/10.1007/s10765-019-2497-1
[22] M. Li, S. Du, Y. Hou, H. Geng, P. Jia, D. Zhao, Study on liquid structure feature of $Al_{100-x}Ni_x$ alloy with resistivity and rapid solidification method, J. Non-Cryst. Solids 411 (2015) 26–34.
https://doi.org/10.1016/j.jnoncrysol.2014.11.031
[23] M. Li, S. Du, R. Liu, S. Lu, P. Jia, H. Geng, Local structure and its change of Al-Ni alloy melts, J. Mol. Liq. 200 (2014) 168–175.
https://doi.org/10.1016/j.molliq.2014.10.007
[24] M. Rappaz, Modelling of microstructure formation in solidification processes, Int. Mater. Rev. 34 (1989) 93–124. doi:10.1179/imr.1989.34.1.93
[25] N. Maraşlı, Ü. Bayram, S. Aksöz, The variations of electrical resistivity and thermal conductivity with growth rate for the Zn-Al-Cu eutectic alloy, J. Mater. Sci. Mater. El. 32 (2021) 18212–18223.
https://doi.org/10.1007/s10854-021-06363-x
[26] M. H. Mulazimoglu, R. Drew, J. E. Gruzleski, The electrical conductivity of cast Al-Si alloys in the range 2 to 12.6 wt pct silicon, Metall. Mater. Trans. A 20 (1989) 383–389.
https://doi.org/10.1007/BF02653917